Evidence for Hydrogen Bond Formation to the PsaB Chlorophyll of P700 in Photosystem I Mutants of *Synechocystis* sp. PCC 6803

Jacques Breton,*,‡ Parag R. Chitnis,§ and Maria Pantelidou§

Service de Bioénergétique, CEA-Saclay, 91191 Gif-sur-Yvette, France, and Department of Biochemistry, Biophysics, and Molecular Biology, Iowa State University, Ames, Iowa 50011

Received December 16, 2004; Revised Manuscript Received February 4, 2005

ABSTRACT: P700, the primary electron donor of photosystem I, is an asymmetric dimer made of one molecule of chlorophyll *a*′ (P_A) and one of chlorophyll *a* (P_B) that are bound to the homologous PsaA and PsaB polypeptides. While the carbonyl groups of P_A are involved in hydrogen-bonding interactions with several surrounding amino acid side chains and a water molecule, P_B does not engage hydrogen bonds with the protein. Notably, the residue Thr A739 is donating a strong hydrogen bond to the 9-keto C═O group of P_A and the homologous residue Tyr B718 is free from interaction with P_B. Light-induced FTIR difference spectroscopy of the photooxidation of P700 has been combined with a site-directed mutagenesis attempt to introduce hydrogen bonds to the carbonyl groups of P_B in *Synechocystis* sp. PCC 6803. The FTIR study of the Y(B718)T mutant provides evidence that the 9-keto C═O group of P_B and P_B^+ engages a relatively strong hydrogen-bonding interaction with the surroundings in a significant fraction (40 ± 10%) of the reaction centers. Additional mutations on the two PsaB residues homologous to those involved in the main interactions between the PsaA polypeptide and the 10a-carbomethoxy groups of P_A affect only marginally the vibrational frequency of the 10a-ester C═O group of P_B. The FTIR data on single, double, and triple mutants at these PsaB sites indicate a plasticity of the interactions of the carbonyl groups of P_B with the surrounding protein. However, these mutations do not perturb the hydrogen-bonding interactions assumed by the 9-keto and 10a-ester C═O groups of P_A and P_A^+ with the protein and have only a limited effect on the relative charge distribution between P_A^+ and P_B^+.

In all photosynthetic organisms, conversion of sunlight into chemical energy occurs in transmembrane pigment−protein complexes called reaction centers (RCs).[1] The RCs of both oxygenic and nonoxygenic organisms exhibit a common general architecture and share the same basic functional principles. Following absorption of a photon, a separation of electric charges takes place between a primary electron donor, a dimer of chlorophyll (Chl) or bacteriochlorophyll molecules, and a series of electron acceptors situated at increasing distances away from the primary donor. Owing to their prominent role in the process of transmembrane separation and stabilization of the electric charges, the electronic structure of the primary donors has been investigated in great detail using various forms of optical, vibrational, and magnetic resonance spectroscopy (*1*). In the case of oxygenic photosynthesis, two large RC complexes, photosystems I and II (PS I and PS II), act in tandem to oxidize water and reduce $NADP^+$. The RCs of PS I and PS II differ predominantly by the nature of their terminal electron acceptor, which is an iron−sulfur protein in type I and a quinone in type II RCs, respectively. The photosynthetic reactions that take place in anoxygenic photosynthetic bacteria involve either type I or type II RCs.

In the last two decades, X-ray crystallographic models of the RC from purple photosynthetic bacteria have provided most valuable information on the structure of the primary donor and the surrounding protein in type II RCs (*1*). Recently, the elucidation of the structure at 2.5 Å resolution of PS I from the cyanobacterium *Synechococcus elongatus* has revealed for the first time many structural details of a type I RC (*2*). Type I and type II RCs share a common pseudo-C_2-symmetry structural motif of several membrane-spanning α-helices within two homologous polypeptides that bind the various redox cofactors. These cofactors are organized in two branches that start at the center of the primary donor and that are also related by the pseudo-C_2-symmetry axis. While electron transfer is known to proceed unidirectionally down along only one branch of cofactors in type II RCs, it has been proposed that both branches would be active in PS I RCs (*3*).

The X-ray structure of PS I at 2.5 Å resolution (*2*) shows interesting features of the asymmetry of the interactions between the primary electron donor (called P700) and the two homologous polypeptides, PsaA and PsaB, that form the core of the RC. Notably, while PsaB binds a Chl *a* molecule (P_B), the Chl bound to PsaA (P_A) is a Chl *a*′ (epimer of Chl *a* at C_{10}) molecule. The structural model also indicates large differences at the level of the bonding interactions

* To whom correspondence should be addressed. Telephone: (331) 6908 2239. Fax: (331) 6908 8717. E-mail: cadara3@dsvidf.cea.fr.
‡ Service de Bioénergétique, CEA-Saclay.
§ Iowa State University.

[1] Abbreviations: Chl, chlorophyll; PS I (II), photosystem I (II); RC, reaction center; P700, primary electron donor of PS I; FTIR, Fourier transform infrared; *Synechocystis*, *Synechocystis* sp. PCC 6803; *C. reinhardtii*, *Chlamydomonas reinhardtii*; *S. elongatus*, *Synechococcus elongatus*.

10.1021/bi0473612 CCC: $30.25
Published on Web 03/09/2005

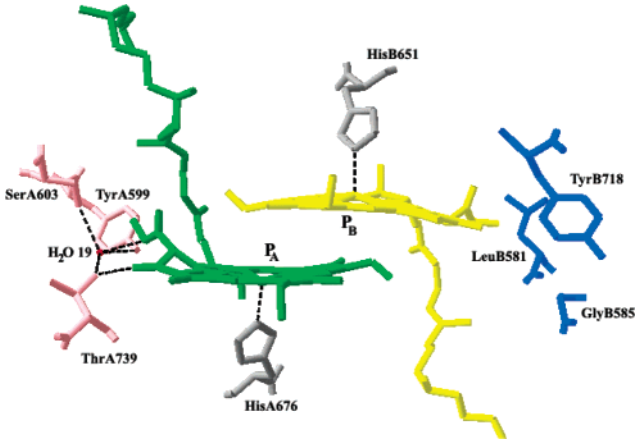

FIGURE 1: Structural model of P700, the primary electron donor of photosystem I derived from the work of Jordan et al. (*2*) on the cyanobacterium *S. elongatus*. General view along the pseudo-C_2 symmetry axis showing the organization of the dimer of chlorophyll *a* (P_B) and chlorophyll *a*′ (P_A) with their central Mg atoms coordinated to the side chains of His B651 and His A676, respectively. Also shown are some of the amino acid residues located in the close vicinity of water H_2O-19 and of the 9-keto and 10a-ester carbonyl groups of P700. Note the residues engaged in putative hydrogen bonds with the carbonyls of P_A and the symmetry-related side chains that appear free from hydrogen-bonding interactions with P_B. The numbering is according to the sequence of the cyanobacterium *Synechocystis* sp. PCC 6803; see Table 1 for a comparison with the sequence of *S. elongatus*.

Table 1: Hydrogen-Bonding Residues of PsaA (and Homologues in PsaB) in *S. elongatus* and *Synechocystis* sp. PCC 6803[a]

S. elongatus		*Synechocystis*	
Tyr A603	Leu B590	Tyr A599	Leu B581
Ser A607	Gly B594	Ser A603	Gly B585
Thr A743	Tyr B727	Thr A739	Tyr B718

[a] Based on the 2.5 Å crystal structure of PS I in *S. elongatus* by Jordan et al. (*2*).

between the carbonyl groups of P_A and P_B and their respective protein partners (see Figure 1). More specifically, residue Thr A739 is proposed to interact both with the 9-keto C═O group of P_A and with a bound water molecule. This water (H_2O-19) appears at the center of a network of hydrogen bonds that involves, in addition to Thr A739, the 10a-carbomethoxy group of P_A and, at least, residues Tyr A599 and Ser A603. The homologous residues on the PsaB side are Tyr B718, Leu B581, and Gly B585, respectively (Figure 1 and Table 1). None of the latter three residues appears to form hydrogen bonds with the carbonyls of P_B. Therefore, it would seem of interest to investigate whether such an asymmetry of the pigment−protein interactions at the level of P700 could be manipulated through site-directed mutagenesis and whether it bears any consequence on the directionality of electron transfer.

Among the spectroscopic techniques that are well suited to investigate the interactions of photochemically active cofactors with the protein binding site, light-induced FTIR difference spectroscopy appears as a choice method (for reviews, see refs *4*−*7*). With regard to the bonding interactions of P700 with the surrounding protein, the conclusion that both the 9-keto and the 10a-ester carbonyl groups of only one of the two Chl molecules of P700 are engaged in hydrogen-bonding interactions with the protein was first reached upon comparing the FTIR difference spectra corresponding to the photooxidation of P700 to $P700^+$ (referred to as $P700^+$/P700 difference spectra in the following) to those for the conversion of P700 to the triplet state ^{3}P700. This comparison led to the assignment of the IR bands corresponding to the upshift upon $P700^+$ formation of the 9-keto and 10a-ester carbonyl C═O groups of each of the two Chl molecules in P700 (*8*). When the X-ray structure of PS I at 2.5 Å resolution appeared (*2*), these assignments could be easily related to the carbonyl groups of P_A, P_A^+, P_B, and P_B^+ (*7*). Note, however, that a divergent assignment has also been proposed for the 9-keto C═O vibrations of P_A and P_A^+ (9).[2] Recently, $P700^+$/P700 FTIR difference spectra were reported for PS I samples bearing mutations that were devised to perturb the hydrogen bond network involving the carbonyl groups of P_A. These mutations were introduced first in *Chlamydomonas reinhardtii* (*12*−*14*) and, more recently, in *Synechocystis* sp. PCC 6803 (hereafter referred to as *Synechocystis*) (*15*). In the latter study, the effect on the $P700^+$/P700 FTIR difference spectra of replacing the three PsaA residues involved in the network of hydrogen bonds (Thr A739, Ser A603, and Tyr A599) by their PsaB homologues (Tyr B718, Gly B585, and Leu B581, respectively) was consistent with the rupture, or at least a significant loosening, of the hydrogen bond to the 9-keto C═O of P_A and with an increased freedom of a bound 10a-ester of P_A (*10*). When only residue Thr A739 was changed to Phe, the perturbation of the hydrogen bond to the 9-keto C═O group of P_A was still observed with almost no changes at the level of the 10a-ester C═O. Very comparable experimental results have been reported in *C. reinhardtii* PS I when Thr A739 was changed to Tyr, His, or Val (*12*) or to Ala (*13*, *14*).

In the present study, we have attempted to perturb the environment of the carbonyl groups of P_B by interchanging either one, two, or three of the PsaB residues Tyr B718, Gly B585, and Leu B581 with their PsaA analogues, and we report on the $P700^+$/P700 FTIR difference spectra of the four mutants that have been obtained by site-directed mutagenesis in *Synechocystis*.

MATERIALS AND METHODS

Site-Directed Mutagenesis. Site-directed mutagenesis of the *psaB* gene was performed using donor plasmid pBC+ that contains the C-terminal region of the *psaB* gene, a 760 bp region downstream of the *psaB* gene, and a chloramphenicol resistance gene (*16*). The site-specific mutations were made using the polymerase chain reaction (PCR) method with platinum *Pfx* polymerase (Invitrogen). The mutated plasmids were checked by sequencing and were used to transform the *Synechocystis* recipient strain, pCRTΔB (a gift from Drs. Jianping Yu and Lee McIntosh, Michigan State University). In this strain the 3′ half of the *psaB* gene was deleted and replaced by a kanamycin resistance gene. The transformants were selected and segregated for several

[2] In our assignment scheme (*7*, *8*, *10*), the 9-keto C═O group of P_A absorbs at 1638 cm^{-1} in *Synechocystis* and upshifts to 1653 cm^{-1} in P_A^+. In the alternative assignment proposed by Hastings and colleagues (9, *11*), the 9-keto C═O group of P_A absorbs at 1695 cm^{-1} and downshifts to 1686 cm^{-1} in P_A^+. In the following, an interpretation of the $P700^+$/P700 FTIR difference spectra of the PsaB mutants within the frame of our assignment scheme will first be presented. It will then be shown that the observed effects of the mutations are inconsistent with the alternative assignment scheme of Hastings and colleagues.

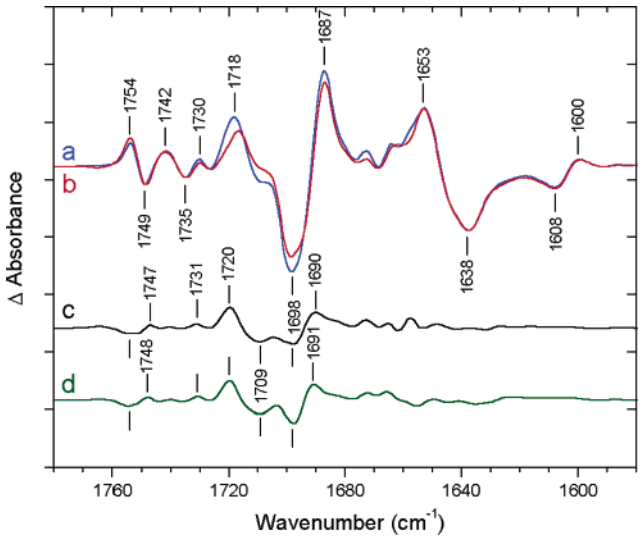

FIGURE 2: Light-induced $P700^+/P700$ FTIR difference spectrum of PS I complexes from *Synechocystis* sp. PCC 6803 at 5 °C: (a) wild-type PS I; (b) mutant G(B585)S; (c) double-difference spectrum, wild-type minus G(B585)S mutant; (d) double-difference spectrum, wild-type minus a double mutant containing the L(B581)Y and G(B585)S changes (see text for details). Each division on the vertical scale corresponds to 1×10^{-3} absorbance unit. About 100000 interferograms were added. The resolution is 4 cm^{-1}, and the frequency of the bands is given ± 1 cm^{-1}.

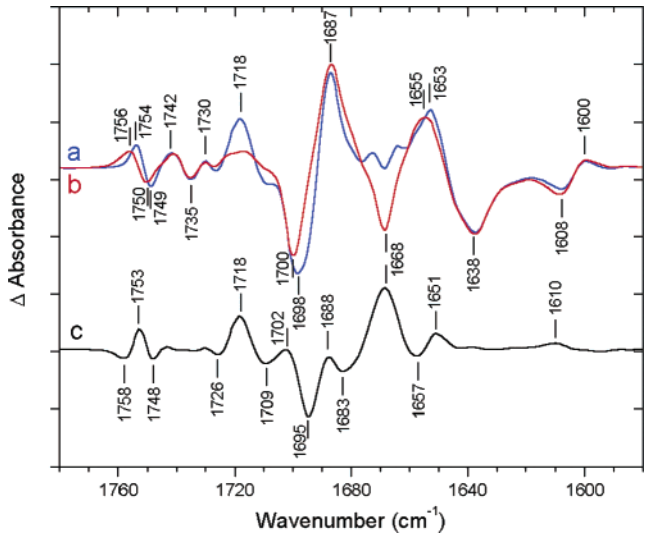

FIGURE 3: Light-induced $P700^+/P700$ FTIR difference spectrum of PS I complexes from *Synechocystis* sp. PCC 6803 at 5 °C: (a) wild-type PS I; (b) single mutant Y(B718)T; (c) double-difference spectrum, wild-type minus Y(B718)T mutant. Each division on the vertical scale corresponds to 1×10^{-3} absorbance unit.

generations on chloramphenicol-supplemented BG11 plates under low light intensity ($2-3$ μmol m^{-2} s^{-1}) at 30 °C. The fragment of interest was amplified from genomic DNA by PCR and sequenced to verify the presence of the desired mutation(s).

Cell Growth and PS I Complex Isolation. Growth of the *Synechocystis* wild-type and mutant strains in BG11 medium was carried out as described previously (*15*). Cells were harvested at mid to late exponential phase (1.0 OD_{730}), and isolation of thylakoid membranes and PS I trimers was carried out as described in ref *17* with minor alterations. PS I trimers at 1 mg/mL Chl concentration were stored at −70 °C.

FTIR Measurements. The IR samples were prepared, and the FTIR measurements were performed as described previously (*15*).

RESULTS

$P700^+/P700$ FTIR Difference Spectrum of the Single Mutant G(B585)S. Figure 2 shows a comparison of the light-induced $P700^+/P700$ FTIR difference spectra of a wild-type control (Figure 2a) and of the mutant G(B585)S (Figure 2b) in the spectral region $1780-1580$ cm^{-1}. The two spectra have been normalized by minimizing the residuals over the spectral range $1800-1200$ cm^{-1} (see Figure 2SI in Supporting Information). The wild-type minus mutant double-difference spectrum is shown (Figure 2c). The two $P700^+/P700$ FTIR difference spectra are remarkably similar in the frequency range below 1660 cm^{-1}. Notably, the differential signal at 1600(+)/1608(−) cm^{-1} assigned to the perturbation upon $P700^+$ formation of the macrocycle C═C marker mode of 5-coordinated Chl (*18*) is unaffected by the mutation. The most significant differences between the two spectra are observed between 1685 and 1725 cm^{-1} in the region of absorption of the 9-keto C═O group of P_B (1698 cm^{-1} for wild-type) and P_B^+ (1718 cm^{-1}) and around 1750 cm^{-1} where the 10a-ester C═O group of P_B (1749 cm^{-1}) and P_B^+ (1754 cm^{-1}) contributes (*7*). The main effect of the mutation on the vibrations of P_B and P_B^+ is a small decrease of the amplitude of the bands assigned to the 9-keto group together with a small increase of the amplitude of the bands attributed to vibrations of the 10a-ester C═O group. The minor bands observed around 1660 and 1550 cm^{-1} (see Figure 2SI in Supporting Information) in the double-difference spectrum can be reasonably assigned to contributions from the protein backbone.

$P700^+/P700$ FTIR Difference Spectrum of the Double Mutant L(B581)Y/G(B585)S. The $P700^+/P700$ FTIR difference spectrum of a double mutant containing the changes L(B581)Y and G(B585)S (data not shown) is actually very close to that of the single G(B585)S mutant, and therefore only the corresponding double-difference spectrum is displayed (Figure 2d). As previously described for the G(B585)S single mutant, the main impact of the mutations on the $P700^+/P700$ FTIR difference spectrum is localized on the bands assigned to the carbonyls of P_B and P_B^+ in wild-type and appears as a slight decrease (increase) of the amplitude of the differential signals assigned to the 9-keto (10a-ester) C═O groups.

$P700^+/P700$ FTIR Difference Spectrum of the Single Mutant Y(B718)T. Figure 3 shows a comparison of the light-induced $P700^+/P700$ FTIR difference spectra of a wild-type control (Figure 3a) and of the single mutant Y(B718)T (Figure 3b) with the double-difference spectrum depicted in Figure 3c. A pronounced effect of the mutation is observed in the spectral region above 1650 cm^{-1} with a number of the bands being strongly affected. However, it is of note that the mutation has little impact on the differential signals previously assigned to the contributions in the spectrum of wild-type of P_A^+/P_A at 1653/1638 cm^{-1} and at 1742/1735 cm^{-1} for the 9-keto and 10a-ester C═O groups, respectively (*7*). On the other hand, the P_B^+/P_B differential signal assigned to the 10a-ester C═O group in wild-type at 1754/1749 cm^{-1} upshifts by $1-2$ cm^{-1}, and its amplitude decreases ap-

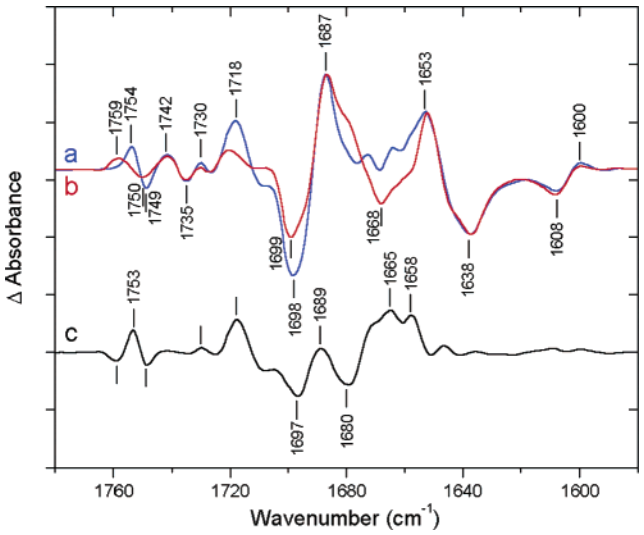

FIGURE 4: Light-induced P700$^+$/P700 FTIR difference spectrum of PS I complexes from *Synechocystis* at 5 °C: (a) wild-type PS I; (b) a triple mutant containing the L(B581)Y, G(B585)S, and Y(B718)T changes; (c) double-difference spectrum, wild-type minus triple mutant. Each division on the vertical scale corresponds to 1 × 10^{-3} absorbance unit.

preciably in the mutant. An even stronger effect of the mutation is observed on the P_B^+/P_B differential signal assigned to the 9-keto C═O group in wild-type at 1718/1698 cm^{-1} with a small downshift (~1 cm^{-1}) and a drastic reduction of the amplitude of the positive component. This is accompanied by a 2 cm^{-1} upshift and a decreased amplitude of the negative band at 1698 cm^{-1}. At lower frequency, a large negative band now appears at 1668 cm^{-1} together with an increase and an apparent broadening of the positive band peaking at 1687 cm^{-1} in the spectrum of wild-type. The amplitude of the 1600(+)/1608(−) cm^{-1} differential signal assigned to the macrocycle C═C marker mode of 5-coordinated Chl is somewhat decreased upon mutation. Both this decrease of amplitude and the alteration of IR bands around 1360−1280 cm^{-1} (see Figure 3SI in Supporting Information) assigned to coupled CC, CN, and CH vibrations of the Chl ring point toward some modification of the conformation of the P_B macrocycle in the Y(B718)T mutant.

P700$^+$/P700 FTIR Difference Spectrum of the Triple Mutant L(B581)Y/G(B585)S/Y(B718)T. Figure 4 shows a comparison of the light-induced P700$^+$/P700 FTIR difference spectra of a wild-type control (Figure 4a) and of a triple mutant containing the changes L(B581)Y, G(B585)S, and Y(B718)T (Figure 4b) with the double-difference spectrum depicted in Figure 4c. In the spectral range above 1670 cm^{-1} the spectrum of the triple mutant (Figure 4b) bears many similarities with that of the single mutant Y(B718)T (Figure 3b), as also evident from the comparison of the corresponding double-difference spectra (Figures 3c and 4c). The main difference between the P700$^+$/P700 FTIR difference spectra of the single mutant (Figure 3b) and of the triple mutant (Figure 4b) resides in an upshift of the positive bands representing the contributions of the 9-keto and 10a-ester C═O groups of P_B^+ in the triple mutant compared to the single Y(B718)T mutant by 3 and 5 cm^{-1}, respectively. The main negative bands at 1698 cm^{-1} in wild-type upshifts by 1 cm^{-1} in the triple mutant. Large differences between the P700$^+$/P700 FTIR spectra of the triple mutant and of the Y(B718)T single mutant are also observed around 1655−1660 cm^{-1}. They are likely to reflect contributions from rearrangements of the protein backbone which could be further investigated by global ^{15}N labeling as shown in a previous study (*15*). More subtle differences between the spectra of these two mutants appear also at many positions as shifts of the frequency of the bands and/or changes in the relative amplitudes of the bands. Notably, the macrocycle C═C marker mode of 5-coordinated Chl responsible for the differential signal at 1600(+)/1608(−) cm^{-1} appears slightly more perturbed in the Y(B718)T single mutant than in the triple mutant. On the other hand, the coupled CC, CN, and CH vibrations giving rise to the IR bands around 1360−1280 cm^{-1} are perturbed in the same way in the two mutants (see Figures 3SI and 4SI in Supporting Information).

DISCUSSION

Effect of the Mutation G(B585)S on the P700$^+$/P700 FTIR Difference Spectra. The impact of the mutation G(B585)S on the P700$^+$/P700 FTIR difference spectra (Figure 2b,c) is both limited and highly specific. It affects mostly the IR bands previously assigned (*7*, *8*) to the 9-keto and 10a-ester carbonyl groups of P_B and P_B^+ without perturbing appreciably those assigned to the carbonyl groups of P_A and P_A^+. The main effect of the mutation is a decrease (by about 15%) of the amplitude of the P_B^+/P_B differential signal assigned to the 9-keto C═O and an increase (by about 10%) of that attributed to the 10a-ester C═O group without any significant shift of frequency of the vibrations. This behavior indicates a change in the environment of the carbonyl groups when the short and apolar side chain of Gly B585 is replaced by the slightly longer and more polar side chain of Ser. The FTIR spectra provide no evidence for the formation of a hydrogen bond between the carbonyl groups of P_B and P_B^+ and the hydroxyl of Ser introduced at the B585 site. The observed changes of relative amplitude of the P_B^+/P_B differential signals are most probably related to the change of polarity of the environment of the carbonyl groups of P_B.

When the effect of the single mutation G(B585)S on the P700$^+$/P700 FTIR difference spectra (Figure 2c) is compared to that of the double mutation L(B581)Y/G(B585)S (Figure 2d), the effect of the additional mutation L(B581)Y is practically unnoticeable. The simplest interpretation is that the Tyr residue introduced at the B581 site points away from the carbonyl groups of P_B and therefore does not perturb the environment of these groups. Indeed, the X-ray structural model of PS I (Figure 1) shows that the side chain of Leu B581 is pointing away from P_B, and it is therefore not surprising that a similar geometry is deduced for the side chain of the Tyr introduced at the B581 site.

Effect of the Mutation Y(B718)T on the P700$^+$/P700 FTIR Difference Spectra. The mutation Y(B718)T has a strong impact on the IR vibrations of the 9-keto and 10a-ester carbonyl groups of P_B and P_B^+. In the region of absorption of the 9-keto C═O group, the two most prominent effects are (i) the pronounced decrease of the amplitude of the 1718/1698 cm^{-1} differential signal assigned to the contribution of the 9-keto C═O in P_B^+/P_B and (ii) the appearance of a large negative band at 1668 cm^{-1} in the spectrum of the mutant. A straightforward interpretation of these changes assumes that the 9-keto C═O group of P_B in the mutant

engages in hydrogen-bonding interaction in a subpopulation of the RCs. For the neutral species, this hydrogen bond would be strong enough to downshift by 27 cm^{-1} the free 9-keto C═O frequency from 1695 to 1668 cm^{-1} (Figure 3c). A direct hydrogen-bonding interaction between the 9-keto C═O group of P_B and the hydroxyl of the introduced Thr side chain does not seem likely from the mere examination of the X-ray structural model (*2*; see also Figure 1). However, interaction via an intervening water molecule could occur, notably upon rotation of the Thr side chain introduced at the B718 site. Furthermore, one cannot exclude that larger rearrangements of the protein, and even some minor displacement of the P_B Chl, in the vicinity of the mutated residue take place, allowing for hydrogen bonding to the 9-keto C═O group of P_B. For the P_B^+ radical corresponding to this subpopulation of P_B, the frequency of the 9-keto C═O group is difficult to extract directly from the FTIR spectra. However, both the broadening of the positive band peaking at 1687 cm^{-1} in the mutant spectrum (Figure 3b) compared to the spectrum of wild-type (Figure 3a) and the shape of the double-difference spectrum (Figure 3c) suggest a distribution of hydrogen bonds of different strengths for this vibration. It is possible that the two negative bands at 1683 and 1695 cm^{-1} in the double-difference spectrum (Figure 3c) correspond to some bimodal distribution of these hydrogen bonds in P_B^+. However, the negative band at 1695 cm^{-1} (Figure 3c) mainly contains the contribution from the 9-keto C═O of P_B in the fraction of the population of wild-type RCs that becomes engaged in hydrogen-bonding interaction upon the Y(B718)T mutation. This overlap hampers a precise determination of the IR frequency of the 9-keto C═O group of P_B^+ in the latter population. Despite this difficulty, the relative amplitudes of the 9-keto C═O differential signals of P_B^+/P_B in the three spectra (Figure 3) allow for a crude estimate of 40 ± 10% for the fractional population of RCs that are engaged in hydrogen-bonding interaction in the Y(B718)T mutant. Note that this estimate relies on the assumption that the extinction coefficient of the carbonyl groups of P_B and P_B^+ is rather insensitive to their hydrogen-bonding state.

Besides the large spectral changes observed in the frequency range of the 9-keto C═O signals of P_B and P_B^+, the other most significant change noted upon the Y(B718)T mutation is the 1−2 cm^{-1} frequency upshift and the amplitude decrease of the P_B^+/P_B differential signal of the 10a-ester C═O group at 1754/1749 cm^{-1}. This change cannot be due to an effect of hydrogen bonding as this would lead to a frequency downshift of the corresponding bands. Most probably, it reflects changes in the conformation and/or environment of the 10a-ester C═O group upon mutation. Although it is commonly thought that the 10a-ester C═O group of Chl *a* is not conjugated to the macrocycle, it has been demonstrated that this is not the case. Indeed, upon generating the Chl a^+ cation in tetrahydrofuran, a C═O ester band absorbing at 1738 cm^{-1} in neutral Chl *a* is upshifted to 1751 cm^{-1} in the cation state, and this set of bands is absent when the experiment is performed with pyroChl *a*, a Chl *a* derivative lacking the 10a-carbomethoxy group (*19*). This observation is actually at the basis of the assignment of the differential signals observed in the range 1730−1760 cm^{-1} of the P700$^+$/P700 FTIR difference spectra to the contributions of the 10a-ester C═O groups of P700 (*19*).

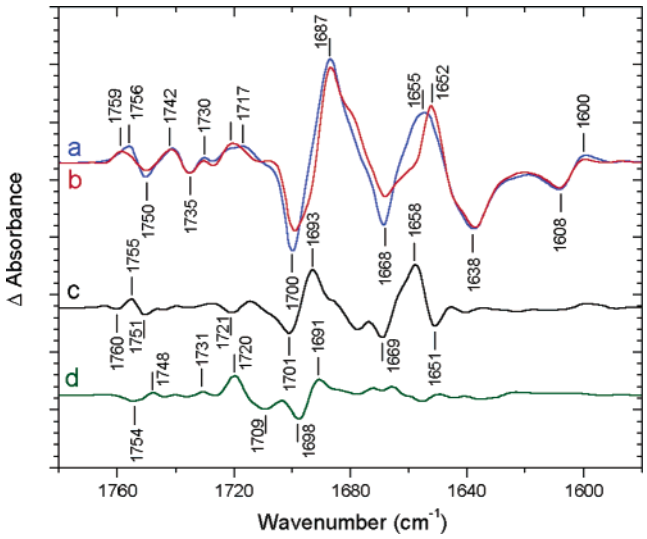

FIGURE 5: Light-induced P700$^+$/P700 FTIR difference spectrum of PS I complexes from *Synechocystis* at 5 °C: (a) single mutant Y(B718)T; (b) the triple mutant containing the L(B581)Y, G(B585)S, and Y(B718)T changes; (c) double-difference spectrum, single mutant Y(B718)T minus triple mutant; (d) double-difference spectrum, wild-type minus the double mutant containing the L(B581)Y and G(B585)S changes (same spectrum as in Figure 2d). Each division on the vertical scale corresponds to 1 × 10^{-3} absorbance unit.

Therefore, the change upon the Y(B718)T mutation of both the amplitude and the frequency of the P_B^+/P_B differential signal of the 10a-ester C═O group at 1754/1749 cm^{-1} (Figure 3) could be well explained by a change of geometry of the 10a-carbomethoxy group. For example, a rotation of the 10a-ester C═O group out of the plane of the ring V of P_B would lead to a decrease of the extent of conjugation of the 10a-ester C═O group to the Chl macrocycle and would induce a shift of the vibrational frequency of this group. Around 1760 cm^{-1}, the high-energy side of the differential signals appears broader for the mutant than for wild-type. This indicates a more heterogeneous distribution of the conformation of the 10a-ester C═O of P_B^+ in the mutant than in wild-type. Another indication of an heterogeneity of the conformation of the P_B Chl is provided by the distribution of frequency of the 1698 cm^{-1} band assigned to its 9-keto C═O group in wild-type (Figure 4a). In the Y(B718)T mutant, this band appears to correspond to two populations of 9-keto carbonyls, a low-frequency one centered around 1695 cm^{-1} which is further downshifted to 1668 cm^{-1} in the mutant (Figure 4c) and another population centered around 1700 cm^{-1} which corresponds to the fraction of the 9-keto groups of P_B that are essentially unaffected by the mutation (Figure 4b).

Effect of the Triple Mutation L(B581)Y/G(B585)S/Y(B718)-T. Upon introducing the triple mutation, the strong decrease of the amplitude of the 1718/1698 cm^{-1} differential signal assigned to the P_B^+/P_B contribution of the 9-keto C═O group and the appearance of a new negative band at 1668 cm^{-1} (Figure 4b) provide evidence to support the conclusion of a new hydrogen-bonding interaction of the 9-keto C═O group of P_B. When the P700$^+$/P700 FTIR difference spectra of the triple mutant and of the single mutant Y(B718)T are compared directly (Figure 5a,b), the many similarities observed above 1670 cm^{-1} further show that it is probably the same partner that is also involved in the hydrogen bond

to the 9-keto C═O group of P_B in the triple mutant. Even in the frequency range above 1745 cm^{-1}, corresponding to the contribution of the 10a-ester C═O group of P_B and P_B^+, the effect of the triple mutation (Figure 4c) resembles more closely that observed in the single Y(B718)T mutant (Figure 3c) than that found in the double mutant L(B581)Y/G(B585)S (Figure 2d), indicating that the impact of the Y(B718)T mutation dominates the spectrum of the triple mutant. The FTIR spectra lend no evidence for hydrogen bond formation with the 10a-ester C═O group of P_B or P_B^+ in the triple mutant.

The comparison of the $P700^+$/P700 FTIR difference spectra of wild-type (Figure 3a) with the single Y(B718)T mutant (Figure 3b) or the triple mutant (Figure 4b) provides no evidence that these PsaB-side mutations perturb the strong bonding interactions that exist for the 9-keto and 10a-ester carbonyl groups of P_A and P_A^+ with the protein at the PsaA sites. On the other hand, the changes observed for several IR modes sensitive to the conformation of the Chl macrocycle, notably the coupled CC, CN, and CH vibrations of the Chl ring around 1360−1280 cm^{-1} (see Figures 3SI, 4SI, and 5SI in Supporting Information) and the C═C marker mode of 5-coordinated Chl around 1600 cm^{-1}, point toward a modification of the conformation of the P_B macrocycle in the Y(B718)T mutant. However, the observed changes are not as pronounced as those occurring upon perturbation of the strong hydrogen bond between Thr A739 and the 9-keto C═O group of P_A (*15*).

It is instructive to compare the effect of introducing the double mutation L(B581)Y/G(B585)S either in wild-type or in the single Y(B718)T mutant on the $P700^+$/P700 FTIR difference spectra. Figure 5c shows the double-difference spectrum calculated by subtracting the spectrum of the triple mutant from that of the single Y(B718)T mutant. This spectrum bears no resemblance to that calculated from the spectra of wild-type and of the L(B581)Y/G(B585)S double mutant (Figure 5d, same as Figure 2d), and therefore it can be concluded that in the triple mutant the effect of the single mutation Y(B718)T and of the double mutation L(B581)Y/G(B585)S is not additive. This observation suggests some specific rearrangements of at least the three side chains introduced upon mutation, and possibly of water molecules, in the triple mutant. For example, one may speculate that a bound water molecule in hydrogen-bonding interactions with the 9-keto C═O group of P_B and the side chain OH group of Thr B718 would rearrange in the triple mutant to interact also with the side chain of Ser B585.

The Effect of the Mutation Y(B718)T Is Inconsistent with the Assignment Scheme of Hastings and Colleagues. The comparison of the $^3P700$/P700 and $P700^+$/P700 FTIR difference spectra (*8*), together with the high-resolution X-ray structure of PS I (*2*), led to the assignment of the 9-keto and 10a-ester C═O groups of P_A, P_A^+, P_B, and P_B^+ (*7*). From these FTIR experiments, it was further concluded that the triplet state is fully localized on P_A and that the positive charge in $P700^+$ is approximately equally shared between P_A and P_B (*7*, *8*). Both of these conclusions were in sharp disagreement with the conclusions from magnetic resonance spectroscopy experiments which were interpreted to provide evidence that both the triplet state in $^3P700$ and the excess spin density in $P700^+$ were essentially localized on P_B (for a review, see ref *20*). This large discrepancy between the interpretation of the results of magnetic resonance and FTIR experiments led Hastings et al. (*9*) to reanalyze the $P700^+$/P700 FTIR difference spectra of *C. reinhardtii* and to propose an assignment of bands for the 9-keto C═O group of P_A that is more consistent with the conclusions derived from magnetic resonance spectroscopy (*20*)[3] but that differs considerably from the previous interpretation of the FTIR data (*7*, *8*). However, the FTIR assignments of Hastings et al. (*9*) are based on the perturbation of the 9-keto carbonyl frequency in a single mutant modified at the His axial ligand of P_A by replacement with a Ser side chain, and they do not take into account the comparison of the $P700^+$/P700 and $^3P700$/P700 FTIR difference spectra that was at the root of the previous assignments (*8*). On the other hand, the $P700^+$/P700 FTIR difference spectra of *C. reinhardtii* and of *Synechocystis* are close enough in the frequency range of absorption of the 10a-ester and 9-keto C═O vibrations of Chl (*7*−*9*, *11*, *12*) that any interpretation of the $P700^+$/P700 FTIR differential signals in terms of detailed bonding interactions should be valid for both species.

In the scheme of Hastings et al. (*9*), the 10a-ester C═O groups of P_A and P_B as well as the 9-keto C═O of P_B all upshift in frequency upon $P700^+$ formation and receive the same assignment as in our previous work (*7*, *8*). On the other hand, the 9-keto C═O of P_A is proposed to absorb around 1695 cm^{-1} and to downshift to 1686 cm^{-1} in P_A^+. No explanation was provided for the physical process underlying this downshift of a Chl 9-keto C═O vibration upon $P700^+$ formation, a behavior that has never been reported when cations of Chl or bacteriochlorophyll are generated either in vivo or in vitro. In their scheme, the large negative band at around 1698 cm^{-1} of wild-type P700 is assigned to the overlap of the 9-keto C═O of both P_A at around 1695 cm^{-1} and P_B at around 1703 cm^{-1} (*9*, *13*, *14*). Although the precise value of the splitting between the peak positions of the 9-keto C═O of P_A and P_B has somewhat varied (between 3 and 9 cm^{-1}) depending on the details of the curve fitting analysis or on the species investigated (*9*, *11*, *13*, *14*), one of the essential characteristics of the model propounded by Hastings et al. (*9*) is that the 9-keto C═O group of P_A in wild-type absorbs at lower frequency than that of P_B.

At first glance, it may seem that the FTIR data on the Y(B718)T mutant (Figure 3) are compatible with the assignment scheme of Hastings et al. (*9*) insofar as the amplitude of both the 1698 cm^{-1} negative band and the associated 1718 cm^{-1} positive band is appreciably decreased in the mutant as would be roughly expected from a downshift upon mutation of the bands assigned to P_B and P_B^+ in wild-type (*9*). A closer inspection of the spectra, however, reveals that the frequency of the bands observed in the spectra (Figure 3) is incompatible with the assignment propounded by Hastings et al. (*9*). Within the frame of their assignment scheme, one would expect the Y(B718)T mutation to induce a downshift of P_B, i.e., of the high-frequency component of the 1698 cm^{-1} negative band of wild-type, therefore leaving a band at lower frequency in the mutant spectrum. This is

[3] Note that the earlier conclusions on the localization of the charge in $P700^+$ and of the triplet character in $^3P700$ from magnetic resonance spectroscopy (*20*) are evolving recently in favor of models (*12*, *14*, *21*) that are more compatible with the conclusions derived from the FTIR experiments (*8*).

just the opposite of what is experimentally observed (Figure 3) where the 1698 cm^{-1} band of wild-type (Figure 3a) is replaced by a band at 1700 cm^{-1} in the Y(B718)T mutant (Figure 3b) while the band affected by the mutation is found at 1695 cm^{-1} (Figure 3c). The same trend for the shifts of the 9-keto C═O frequencies is also observed in the case of the triple mutant, although the magnitude of the shifts is somewhat smaller. Therefore, our observations on the effect of the Y(B718)T mutation on the $P700^+$/P700 FTIR difference spectra cannot be reconciled with the assignment scheme of Hastings and colleagues (*9*, *11*, *13*, *14*).

CONCLUSIONS

The present FTIR study shows that the Y(B718)T mutation leads to hydrogen bonding of the 9-keto C═O group of P_B and P_B^+ in a significant fraction of the centers. On the other hand, the mutations L(B581)Y and G(B585)S have only a small impact on the $P700^+$/P700 FTIR difference spectra. None of these three mutations perturb the hydrogen-bonding interactions assumed by the 9-keto and 10a-ester carbonyl groups of P_A and P_A^+ with the protein. These mutations have only a limited effect on the relative charge distribution between P_A^+ and P_B^+. While the data are consistent with the notion of some plasticity for the interactions of the carbonyls of P_B with the surrounding protein, they also demonstrate that the strong hydrogen-bonding interactions that exist between the 9-keto and 10a-ester carbonyl groups of P_A and three key residues of PsaA cannot be duplicated on the PsaB side by simply replacing the corresponding amino acid residues by their PsaA homologues. A larger set of mutants, notably those involving a swap between the residues at the three sites of the PsaA and PsaB polypeptides investigated in the present study, would help to map out the plasticity of the molecular interactions of the carbonyl groups of P700 with the protein and to study their possible influence on the directionality of electron transfer in PS I.

ACKNOWLEDGMENT

The authors thank G. Ajlani, E. Nabedryk, and W. Xu for stimulating discussions.

SUPPORTING INFORMATION AVAILABLE

Light-induced $P700^+$/P700 FTIR difference spectra (Figures 2SI−5SI) in the spectral range 1800−1200 cm^{-1}. This material is available free of charge via the Internet at http://pubs.acs.org.

REFERENCES

1. Hoff, A. J., and Deisenhofer, J. (1997) Photophysics of photosynthesis: Structure and spectroscopy of reaction centers of photosynthetic bacteria, *Phys. Rep. 287*, 1−247.
2. Jordan, P., Fromme, P., Witt, H. T., Klukas, O., Saenger, W., and Krauss, N. (2001) Three-dimensional structure of cyanobacterial photosystem I at 2.5 Å resolution, *Nature 411*, 909−917.
3. Guergova-Kuras, M., Boudreaux, B., Joliot, A., Joliot, P., and Redding, K. (2001) Evidence for two active branches in photosystem I, *Proc. Natl. Acad. Sci. U.S.A. 98*, 4437−4442.
4. Mäntele, W. (1993) Infrared vibrational spectroscopy of the photosynthetic reaction center, in *The Photosynthetic Reaction Center* (Deisenhofer, J., and Norris, J. R., Eds.) Vol. II, pp 239−283, Academic Press, San Diego.
5. Nabedryk, E. (1996) Light-induced Fourier transform infrared difference spectroscopy of the primary electron donor in photosynthetic reaction centers, in *Infrared Spectroscopy of Biomolecules* (Mantsch, H. H., and Chapman, D., Eds.) pp 39−81, Wiley-Liss, New York.
6. Breton, J., and Nabedryk, E. (1996) Protein-quinone interactions in the bacterial photosynthetic reaction center: Light-induced FTIR difference spectroscopy of the quinone vibrations, *Biochim. Biophys. Acta 1275*, 84−90.
7. Breton, J. (2001) Fourier transform infrared spectroscopy of primary electron donors in type I photosynthetic reaction centers, *Biochim. Biophys. Acta 1507*, 180−193.
8. Breton, J., Nabedryk, E., and Leibl, W. (1999) FTIR study of the primary electron donor of photosystem I (P700) revealing delocalization of the charge in $P700^+$ and localization of the triplet character in ^{3}P700, *Biochemistry 38*, 11585−11592.
9. Hastings, G., Ramesh, V. M., Wang, R., Sivakumar, V., and Weber, A. (2001) Primary donor photo-oxidation in photosystem I: A re-evaluation of ($P700^+$ − P700) Fourier transform infrared difference spectra, *Biochemistry 40*, 12943−12949.
10. Breton, J., Xu, W., Diner, B. A., and Chitnis, P. (2002) The two histidine axial ligands of the primary electron donor chlorophylls (P700) in photosystem I are similarly perturbed upon $P700^+$ formation, *Biochemistry 41*, 11200−11210.
11. Wang, R., Sivakumar, V., Johnson, T. W., and Hastings, G. (2004) FTIR difference spectroscopy in combination with isotope labeling for identification of the carbonyl modes of P700 and $P700^+$ in photosystem I, *Biophys. J. 86*, 1061−1073.
12. Witt, H., Schlodder, E., Teutloff, C., Niklas, J., Bordignon, E., Carbonera, D., Kohler, S., Labahn, A., and Lubitz, W. (2002) Hydrogen bonding to P700: Site-directed mutagenesis of threonine A739 of photosystem I in *Chlamydomonas reinhardtii*, *Biochemistry 41*, 8557−8569.
13. Wang, R., Sivakumar, V., Li, Y., Redding, K., and Hastings, G. (2003) Mutation induced modulation of hydrogen bonding to P700 studied using FTIR difference spectroscopy, *Biochemistry 42*, 9889−9897.
14. Li, Y., Lucas, M.-G., Konovalova, T., Abbott, B., MacMillan, F., Petrenko, A., Sivakumar V., Wang, R., Hastings, G., Gu, F., van Tol, J., Brunel, L.-C., Timkovich, R., Rappaport, F., and Redding, K. (2004) Mutations of the putative hydrogen-bond donor to P700 of photosystem I, *Biochemistry 43*, 12634−12647.
15. Pantelidou, M., Chitnis, P., and Breton, J. (2004) FTIR spectroscopy of *Synechocystis* 6803 mutants affected on the hydrogen bonds to the carbonyl groups of the PsaA chlorophyll of P700 supports a model of extensive delocalization of the charge in $P700^+$, *Biochemistry 43*, 8380−8390.
16. Cohen, R. O., Shen, G., Golbeck, J. H., Xu, W., Chitnis, P., Valieva, A. I., van der Est, A., Pushkar, Y., and Stehlik, D. (2004) Evidence for asymmetric electron transfer in cyanobacterial photosystem I: Analysis of a methionine-to-leucine mutation of the ligand to the primary electron acceptor A_0, *Biochemistry 43*, 4741−4754.
17. Sun, J., Ke, A., Jin, P., Chitnis, V. P., and Chitnis, P. R. (1998) Isolation and functional studies of Photosystem I subunits in the cyanobacterium *Synechocystis* sp. PCC 6803, *Methods Enzymol. 297*, 124−139.
18. Fujiwara, M., and Tasumi, M. (1986) Metal-sensitive bands in the Raman and infrared spectra of intact and metal-substituted chlorophyll *a*, *J. Phys. Chem. 90*, 5646−5650.
19. Nabedryk, E., Leonhard, M., Mäntele, W., and Breton, J. (1990) Fourier transform infrared spectroscopy provides no evidence for an enolization of chlorophyll *a* upon cation formation either in vitro or during P700 photooxidation, *Biochemistry 29*, 3242−3247.
20. Weber, A. N., and Lubitz, W. (2001) P700: the primary electron donor of photosystem I, *Biochim. Biophys. Acta 1507*, 61−79.
21. Plato, M., Krauss, N., Fromme, P., and Lubitz, W. (2003) Molecular orbital studies of the primary electron donor P700 of photosystem I based on a recent X-ray single-crystal analysis, *Chem. Phys. 294*, 483−499.

BI0473612